Vol. 601: 59–76, 2018
https://doi.org/10.3354/meps12639

MARINE ECOLOGY PROGRESS SERIES
Mar Ecol Prog Ser

Published August 9

Calcification of an estuarine coccolithophore increases with ocean acidification when subjected to diurnally fluctuating carbonate chemistry

Meredith M. White[1,3], David T. Drapeau[1], Laura C. Lubelczyk[1], Victoria C. Abel[2], Bruce C. Bowler[1], William M. Balch[1,*]

[1]Bigelow Laboratory for Ocean Sciences, East Boothbay, ME 04544, USA
[2]Colby College, Waterville, ME 04901, USA

[3]*Present address:* Mook Sea Farm, Walpole, ME 04573, USA

ABSTRACT: Ocean acidification has the capacity to impact future coccolithophore growth, photosynthesis, and calcification, but experimental culture work with coccolithophores has produced seemingly contradictory results and has focused on open-ocean species. We investigated the influence of pCO_2 (between 250 and 750 µatm) on the growth, photosynthetic, and calcification rates of the estuarine coccolithophore *Pleurochrysis carterae* using a CO_2 manipulation system that allowed for natural carbonate chemistry variability, representing the highly variable carbonate chemistry of coastal and estuarine waters. We further considered the influence of pCO_2 on dark calcification. Increased pCO_2 conditions had no significant impact on *P. carterae* growth rate or photosynthetic rate. However, *P. carterae* calcification rates significantly increased at elevated mean pCO_2 concentrations of 750 µatm. *P. carterae* calcification was somewhat, but not completely, light-dependent, with increased calcification rates at elevated mean pCO_2 conditions in both light and dark incubations. This trend of increased calcification at higher pCO_2 conditions fits into a recently developed substrate-inhibitor concept, which demonstrates a calcification optima concept that broadly fits the experimental results of many studies on the impact of increased pCO_2 on coccolithophore calcification.

KEY WORDS: Ocean acidification · Coccolithophore · Calcification · Carbon dioxide · CO_2 · Photosynthesis · PIC:POC ratio · *Pleurochrysis carterae*

INTRODUCTION

The global ocean is currently undergoing rapid environmental changes due to anthropogenic activities. One change of great concern has emerged largely in the last decade, namely ocean acidification (OA) driven by increased atmospheric carbon dioxide (Doney et al. 2009). When CO_2 enters the ocean, it reacts with water to form carbonic acid and ultimately increases the bicarbonate (HCO_3^-) concentration, decreases the carbonate (CO_3^{2-}) concentration, decreases pH, and decreases the calcium carbonate saturation state ($\Omega_{calcite}$), which may have negative implications for calcifying organisms. Culture experiments investigating the impacts of OA on coccolithophore photosynthesis and calcification have shown contradictory results among species and even among strains of the same species (Riebesell et al. 2000, Langer et al. 2006, 2009, Iglesias-Rodriguez et al. 2008, Hoppe et al. 2011). While some work shows negative impacts of OA between pCO_2 values of ~300 and 750 ppmv on coccolithophore calcification

*Corresponding author: bbalch@bigelow.org

(Riebesell et al. 2000, Langer et al. 2009, Hoppe et al. 2011), other work shows no impact of increasing pCO_2 on coccolithophores (Langer et al. 2006), a non-linear response (Langer et al. 2006, Hoppe et al. 2011), and positive responses with increasing pCO_2 (Iglesias-Rodriguez et al. 2008). Additionally, field observations show that coccolithophore concentrations in the North Atlantic have increased up to 20% from 1965 to 2010, with increased CO_2 as one of the 2 best predictors of change (Rivero-Calle et al. 2015, Krumhardt et al. 2016). Recently, a novel 'substrate-inhibitor concept' has been proposed as a unifying framework that describes these variable responses among species and strains (Bach et al. 2015). The majority of culture experiments have focused on open-ocean species, which are naturally exposed to less variable CO_2 conditions, with only 2 studies considering the estuarine coccolithophore species *Pleurochrysis carterae* (Casareto et al. 2009, Moheimani & Borowitzka 2011), despite its importance as a model organism for coccolithophore biocalcification, crystal growth, and ultrastructure (de Vrind-de Jong et al. 1986, de Vrind-de Jong & de Vrind 1997, Marsh 1999, 2008).

Coastal and estuarine carbonate chemistry conditions are highly variable on time scales ranging from diurnal to seasonal (Cai et al. 2011, Wallace et al. 2014, Baumann et al. 2015). Diel variability in carbonate chemistry is produced by changes in net community photosynthesis and respiration, with lower pCO_2 (higher pH) during the day when there is net photosynthesis, and higher pCO_2 (lower pH) during the night when there is net respiration. This diel pH range can be as high as 0.7 pH units in salt marshes (Baumann et al. 2015). Seasonal variability is driven largely by seasonal phytoplankton blooms resulting from eutrophication, leading to elevated pCO_2 conditions in stratified bottom waters where microbial respiration breaks down the organic matter from the blooms, producing a seasonal pH range of up to 0.6 pH units (Cai et al. 2011). Therefore, organisms living in coastal and estuarine waters are already exposed to carbonate chemistry variability that exceeds the projected open-ocean change in the next 100 yr (Caldeira & Wickett 2003).

Moreover, diurnally fluctuating carbonate chemistry appears to have different effects on coastal diatoms than on oceanic diatoms. For example, the coastal diatom *Thalassiosira weissflogii* showed either enhancement (or no change) in physiological performance under diurnally varying carbonate chemistry, whereas the oceanic diatom *T. oceanica* was significantly negatively affected by diurnally varying carbonate chemistry (Li et al. 2016). The majority of OA perturbation experiments have been performed using relatively stable pH conditions, but recently, calls have been made for OA experimental conditions that allow for natural variability of CO_2 to more accurately represent the conditions that species experience in the wild (McElhany & Busch 2013, Gledhill et al. 2015).

OA has the potential to affect multiple physiological processes in coccolithophores, including growth rate, photosynthetic rate, calcification, and photoregulation. If a coccolithophore species is currently experiencing carbon limitation under ambient pCO_2 conditions, an increase in pCO_2 may release the species from carbon limitation, potentially increasing its growth and photosynthetic rates (Winter et al. 2014, Hermoso et al. 2016). In contrast, calcification is already an energy-intensive process (Brownlee & Taylor 2004, Monteiro et al. 2016), and calcification in water with a reduced saturation state due to OA becomes increasingly energetically costly for organisms, even when the water remains supersaturated (Orr et al. 2005).

The light-dependency of calcification in coccolithophores can be indicative of the energy source used for calcification. Calcification in the dark would require respiratory energy, while complete light-dependency of calcification indicates a requirement for photosynthetic energy (de Vrind-de Jong & de Vrind 1997). While calcification in the well-studied open-ocean coccolithophore *Emiliania huxleyi* is light-dependent (Paasche 1962, Linschooten et al. 1991, Nimer & Merrett 1993), calcification in *P. carterae* can occur in the dark (van der Wal et al. 1987), indicating that *P. carterae* uses at least some respiratory energy for calcification. This use of limited respiratory energy may be affected by OA due to changes in both seawater $\Omega_{calcite}$ and $[H^+]$. In addition to the increased energetic cost of calcifying in lower $\Omega_{calcite}$ water, intracellular coccolith calcification produces H^+, which must be transported out of the cells to prevent cytosol acidification (Brownlee et al. 1994). Increasing seawater $[H^+]$ resulting from OA may impair the efflux of H^+ by reducing the electrochemical gradient between the cytosol and seawater (Taylor et al. 2011, 2012). As such, the energetic cost of calcification at higher CO_2 levels may increase, to the extent that dark calcification may be impaired. Moreover, there can be synergistic effects between light and OA on the growth of coccolithophores. For example, at low irradiance levels, OA can show a negative effect on growth and calcification of *E. huxleyi*, while at high light levels, OA has no effect, sug-

gesting that under sufficient illumination, this can offset the impact of OA (Jin et al. 2017).

In order to better understand the response of an estuarine coccolithophore to an increase in the mean seawater pCO_2 due to increasing atmospheric CO_2, we designed a laboratory OA perturbation study in which we raised *P. carterae* under 3 mean atmospheric pCO_2 conditions: 280, 380, and 750 µatm pCO_2, representing pre-industrial, near-ambient, and projected year 2100 (720–1000 ppmv; Representative Concentration Pathway [RCP]8.5 scenario, IPCC 2014), respectively. The experimental system manipulated only the pCO_2 of the equilibrating air, allowing the algae to exert biological control on the carbonate chemistry system, which produced variable conditions representing natural variability. Our work tests the hypotheses that the growth and photosynthetic rates of *P. carterae* will increase and that the overall calcification rate and dark calcification rates of *P. carterae* will decrease under naturally variable, but elevated, pCO_2 conditions. We interpret our results in the context of the recently proposed substrate-inhibitor concept for coccolithophore sensitivity to OA (Bach et al. 2015).

MATERIALS AND METHODS

Culture conditions

Pleurochrysis carterae cultures (NCMA strain 645; coastal isolate from Nantucket Sound, MA, USA; 1958) were maintained in semi-continuous batch culture using 20 l polycarbonate carboys containing L1-Si culture media (Guillard & Hargraves 1993). Cultures were axenic (verified using bacterial test media incubations [Andersen 2005] as well as light microscopy). Media were prepared in 0.2 µm-filtered, UV-sterilized, autoclaved seawater. Cultures and prepared media were bubbled through a fine glass frit immersed in the media at about 500 ml min^{-1} with 0.2 µm-filtered 280, 380, or 750 µatm pCO_2 in air. The pCO_2 levels of the treatment air were established using 2 mass flow controllers (Aalborg) for each treatment to precisely mix in-house compressed air and pure CO_2. The in-house compressed air was stripped of CO_2 to less than 10 µatm CO_2 using a Puregas VCD CO_2 Adsorber. The pCO_2 level of each mixture was periodically checked using an LI-820 CO_2 Gas Analyzer (LI-COR Biosciences) calibrated with 200 and 1000 µatm CO_2 standard gasses (Scott-Marin), and the CO_2 treatments were found to be stable to ±8 µatm. This manipulation technique controlled only the pCO_2 of the incoming air to the culture, not the CO_2 concentration of the culture itself, and therefore the CO_2 concentration of the cultures varied around the target levels due to biological activity.

Cultures were maintained at 16.5 ± 0.5°C and 470 µmol photons m^{-2} s^{-1} photosynthetically active radiation (PAR) on a 14:10 h light:dark cycle. The relatively high light level was chosen so as to minimize the possibility of light limitation of growth. During culture maintenance, cell density and cell diameter were measured daily (from 10:00–11:00 h) using a Moxi Z mini automated cell counter (ORFLO Technologies) with counts validated using hemocytometer counts. *In vivo* fluorescence was measured daily using a Turner 10-AU fluorometer (Turner Designs). Cultures were maintained in exponential growth by dilutions about every 5–7 d using CO_2-equilibrated media as soon as cultures neared the end of the exponential phase. Exponential phase was determined based on the linearity of a semi-logarithmic plot of cell abundance versus time. For these experiments, the least-squares fit of the log of cell abundance versus time showed an r^2 value >0.95 during any period of exponential growth. Specific growth rates (µ, in units of d^{-1}) for 2 time points, t_n and t_{n+1}, were calculated from cell density at t_n and t_{n+1} as:

$$\mu = \frac{\ln\left[(\text{cell density})_{t_{n+1}} / (\text{cell density})_{t_n}\right]}{(t_{n+1} - t_n)} \quad (1)$$

No experimental data were collected until the cultures had been growing for at least 9 generations, which is recommended for well-acclimated cultures (LaRoche et al. 2010). We note, however, that there has been little evidence that pCO_2 exposures over >150 generations have any different effect than exposures over shorter durations (Barcelos e Ramos et al. 2010, Müller et al. 2010).

Characterization of carbonate chemistry and biogeochemical variables

During routine culture maintenance, the pH of each pCO_2 treatment culture was measured daily using an Orion ROSS™ electrode connected to an Orion Star™ A211 Benchtop pH meter (Thermo-Fisher Scientific), calibrated with National Bureau of Standards (NBS) buffers (EK Industries) and corrected to the total scale using weekly spectrophotometric pH measurements of culture samples. Spectrophotometric pH measurements of 0.2 µm-filtered

culture samples were made with 20 mM *m*-cresol purple sodium salt indicator dye (Alfa Aesar) using a Hitachi U-3010 spectrophotometer (Hitachi High-Technologies) equipped with a water-circulated cell holder connected to a VWR 1160 water bath set at 16.5°C, holding a 1 cm quartz cell. The method followed the procedure described by Clayton & Byrne (1993) and Dickson et al. (2007), using the refit equation of Liu et al. (2011), resulting in a resolution of ±0.004 pH units.

In order to fully characterize the chemistry of the cultures over various time scales, we took single samples for cell density, cell diameter, *in vivo* fluorescence, pH, total alkalinity (A_T; in triplicate), temperature, salinity, nitrate, phosphate, silicate, particulate inorganic carbon (PIC), and particulate organic carbon (POC) from each pCO_2 treatment daily between 10:00 and 11:00 h throughout several complete batch culture growth cycles, from log to stationary phase (14 d). Descriptions of analyses and calculations are below. Additionally, for one 24 h period, we made hourly measurements of each of the above-mentioned parameters, with the exception of POC, for each pCO_2 concentration. Due to sampling time constraints, A_T was measured only every 3 h instead of hourly. The cell density during this 24 h experiment began at ~50 000 cells ml^{-1}.

Culture samples for nutrient and A_T analyses were filtered through 0.2 µm pore size, 25 mm diameter, polycarbonate filters to remove all algal cells and coccoliths. Nutrient samples were frozen prior to analysis. A_T was measured via titration with 0.01 N HCl using a Metrohm Titrando 888 controlled by Tiamo software (Metrohm) to perform automated Gran titrations of 4 ml samples. Titrations were corrected to Certified Reference Material Batches 128 and 132 (supplied by the laboratory of Andrew Dickson, Scripps Institution of Oceanography, La Jolla, CA, USA) and had a precision of 7.7 µequiv kg^{-1}. Salinity was measured using an Acorn SALT 6 handheld salinity meter (Oakton Instruments) with a resolution of ±0.1. Nutrients (nitrate + nitrite, nitrite, phosphate, and silicate) were measured by colorimetric techniques (Parsons et al. 1984) at the University of California, Santa Barbara, Marine Science Institute's Analytical Lab using a QuikChem 8000 (Lachat Instruments) or by continuous flow analysis by Bigelow Analytical Services (East Boothbay, ME, USA) using a SEAL AutoAnalyzer 3 HR (SEAL Analytical). Using the measured values of pH (total scale, pH_T), A_T, temperature, salinity, phosphate, and silicate, we used CO2SYS software (Pierrot et al. 2006) to calculate pCO_2, dissolved inorganic carbon (DIC), $[HCO_3^-]$, $[CO_3^{2-}]$, $[CO_2]$, and $\Omega_{calcite}$ using the first and second dissociation constants (K_1 and K_2) of carbonic acid in seawater from Mehrbach et al. (1987), refit by Dickson & Millero (1987); $KHSO_4$ from Dickson (1990); and total boron concentration ($[B]_T$) from Uppström (1974).

Bulk culture PIC analyses followed the technique of Poulton et al. (2006): 10 ml culture samples were filtered onto 0.4 µm, 25 mm diameter polycarbonate filters and rinsed with potassium borate buffer with the pH adjusted to 8.0 to remove seawater calcium chloride. Filters were carefully transferred to trace metal-free centrifuge tubes and digested with 5 ml of 5% nitric acid. The calcium concentration was measured using a Jobin Yvon Ultima C inductively coupled plasma-atomic emission spectrometer (ICP-AES, HORIBA) at the Boston University Analytical Geochemistry & Geochronology Facilities. To determine the bulk culture POC concentration, 10 ml of culture were filtered onto a pre-combusted Whatman GF/F filter, which was then fumed in 10% HCl to remove inorganic carbonates. Dried filters were then analyzed on an ECS 4010 CHNSO Analyzer (Costech Analytical Technologies) by Bigelow Analytical Services. Bulk culture PIC and POC measurements were corrected to PIC $cell^{-1}$ and POC $cell^{-1}$, respectively, using the corresponding cell density measurements.

Light-dependency of calcification

To determine the light-dependency of *P. carterae* calcification, coccolithophores acclimated to 3 CO_2 concentrations equilibrated with the media (280, 380, and 750 µatm) for >9 generations had their coccoliths removed (i.e. 'de-calcified') following a procedure similar to that described by Balch et al. (1996) and van der Wal et al. (1987). Coccoliths were dissolved by addition of 1.75 M HCl to drop the pH to 5.5 for 2 min. Following the coccolith removal, 1.75 M NaOH was added to bring the pH back to the respective starting pH (8.3). Dissolution of coccoliths was confirmed by viewing the cells under cross-polarized light microscopy to verify the absence of birefringence indicating the absence of $CaCO_3$. For each pCO_2 level, 15 ml of culture containing de-calcified cells were added to 8 borosilicate scintillation vials (analogous to incubation vessels used in photosynthetron experiments; Lewis & Smith 1983). Three vials were 'light' replicates, 3 vials were 'dark' replicates, and 2 vials were poisoned with buffered formalin to serve as a 'light' control and a 'dark' control. All vials were incubated at 16.5 ± 0.5°C. Illuminated

vials were maintained under 470 µmol photons m^{-2} s^{-1} PAR on a 14:10 h light:dark cycle (lights came on at 06:00 h local time). We performed 24 h incubations in order to include a complete light–dark cycle. The experiment was timed to start when the lights in the incubator turned on in the morning, thus the 'light' replicates were exposed to light for 14 of 24 h. During the 24 h experiment, the cells were not bubbled. With 15 ml of sample, the vials were 68% full, with 7 ml of headspace.

Coccolith formation was assessed by counting the number of coccoliths formed during the incubation period. Samples were filtered onto 0.4 µm polycarbonate filters prior to the de-calcifying step, after de-calcifying (to further verify dissolution of coccoliths), and after the 24 h incubation period. Filters were mounted on stubs, sputter-coated with gold using a Denton Desk IV sputter coater (Denton Vacuum), and imaged on a Zeiss Supra25 field emission scanning electron microscope (SEM; Carl Zeiss Microscopy). At least 15 cells $replicate^{-1}$ were imaged and the number of coccoliths $cell^{-1}$ was manually counted (as much as 460 coccoliths in total). The counted coccoliths represented calcification during the 24 h incubation period.

Photosynthetic and calcification rate measurements

Subsamples from cultures of *P. carterae* previously acclimated to 280, 380, and 750 µatm pCO_2 for >9 generations were spiked with $^{14}C\text{-}HCO_3^-$ (MP Biomedicals) and incubated at 16.5 ± 0.5°C and 415 µmol photons m^{-2} s^{-1} PAR for 3 h in order to measure photosynthesis and calcification via the ^{14}C-microdiffusion technique (Paasche & Brubak 1994, Balch et al. 2000). The 3 h incubation was started 3 h into the light period (i.e. at 09:00 h). The 3 h incubation time was chosen to minimize perturbations to the carbonate system during the incubation period due to biological activity. Triplicate cultures for each treatment were not bubbled with their respective pCO_2 treatment during the incubation, since this would have potentially driven off the ^{14}C bicarbonate from the culture into the head space; however, pH was measured before and after the incubation and it did not change significantly. At the end of the incubation, cells from each replicate, along with triplicate formalin-killed blanks for each pCO_2 treatment, were filtered onto 0.4 µm pore size polycarbonate filters, and their carbon was partitioned into organic and inorganic fractions by acidification and subsequent capture of $^{14}CO_2$ (from PIC) in a trap containing a Whatman GFA filter presoaked with 0.2 ml phenethylamine (see Balch et al. 2000 for detailed methodology). The radioactivity of each fraction was measured on a Packard Tri-Carb 2750 LL scintillation counter (acquired by Perkin Elmer), and the photosynthetic rate and calcification rate were calculated from the organic carbon and inorganic carbon fractions, respectively, using the equation of Parsons et al. (1984).

To estimate daily photosynthesis (P_{24}) and calcification (C_{24}) rates from measured 3 h carbon fixation measurements (P_3 and C_3 respectively), we had to correct for the 14:10 h light:dark cycle. We estimated P_{24} by taking the measured P_3 rate, dividing by 0.125 (3/24) to convert to an assumed rate for cells in constant light, then corrected this by the fraction of the day that the cells were illuminated (14/24), as follows:

$$P_{24} = (P_3/3\text{ h}) \times 14\text{ h} \quad (2)$$

The equation for P_{24} (Eq. 2) represents a gross daily photosynthetic rate and does not include dark respiration. Using the data from the calcification light-dependency experiment, for each pCO_2 treatment, we calculated the proportion of calcification in the dark relative to that in the light (x) and used that proportion to determine the corrected 24 h net calcification rate (C_{24}) of *P. carterae.*

$$C_{24} = (C_3/3\text{ h}) \times 14\text{ h} + C_3/3\text{ h} \times 10\text{ h} \times x \quad (3)$$

Gross photosynthetic and net calcification rates (P_{24} and C_{24}) in units of µg C l^{-1} d^{-1} were then normalized to cell density of the respective culture and had unit conversions to determine final daily, cellular photosynthetic, and calcification rates P and C, respectively (units pmol C $cell^{-1}$ d^{-1}). The PIC:POC production ratios of the cells were determined by dividing the daily net calcification rate by the daily net photosynthetic rate.

Statistical analyses

Statistical analyses were performed using SYSTAT 13 (Systat Software). Culture dynamics and chemistry over the 24 h period and 14 d period were analyzed using 1-way ANOVAs with pCO_2 treatment as the factor and using time points as replicates. Growth rate was analyzed using a 2-way ANOVA with pCO_2 treatment and growth cycle as the 2 factors. Calcification rate (coccoliths formed $cell^{-1}$ 24 h^{-1}) during the light/dark experiment was analyzed using a 2-way ANOVA with pCO_2 and light treatment as the 2 factors. Daily net photosynthetic and calcification rates

measured by the ^{14}C-microdiffusion technique, as well as PIC:POC ratios were analyzed using 1-way ANOVAs with pCO_2 treatment as the factor. ANOVAs showing a significant difference ($p < 0.05$) among the 3 pCO_2 treatments were followed by Tukey's post hoc test to identify which treatment(s) were significantly different from each other.

RESULTS

Culture chemistry and cellular dynamics

Our method of precisely controlling the pCO_2 of incoming gas, but not the pCO_2 of the culture itself, resulted in culture biogeochemical processes (photosynthesis, respiration, and calcification) affecting the carbonate chemistry of the 3 treatments (Table 1, Figs. 1 & 2). Mean culture chemistry conditions, representing variability experienced during a diel cycle and over a growth cycle (covering exponential growth and early stationary phase), showed that the 280 and 380 µatm culture treatments were not significantly different from each other, although both culture treatments were significantly different from the 750 µatm culture treatment with respect to pH_T, pCO_2, $[CO_3^{2-}]$, $[CO_2]$, and $\Omega_{calcite}$ (Tables 1 & 2). No significant differences were found among culture treatments with respect to salinity, alkalinity, phosphate, silicate, DIC, or $[HCO_3^-]$. The temperature was significantly different between the different culture treatments (1-way ANOVA, $F_2 = 3.14$, $p = 0.047$; Tables 1 & 2) (well within the range of the variability of the incubator), but Tukey's post hoc test did not show a significant difference among any pairs of culture treatments, which may be due to the more stringent criteria for significance of the post hoc test, relative to the ANOVA (Sokal & Rohlf 1995). In contrast, the pCO_2 treatments of media only (no algae) showed significant differences between each treatment level with respect to pH_T, pCO_2, $[CO_2]$, and $\Omega_{calcite}$ (Table 1), indicating it was indeed biological activity that caused the carbonate chemistry of the 280 and 380 µatm culture treatments to be statistically similar to each other.

The carbonate chemistry conditions of the cultures varied over the course of a day (Fig. 1, Table 1), due to changes in productivity and respiration, and over the course of a growth cycle (Fig. 2, Table 1), due to increasing biomass and $CaCO_3$ during that time. Over a 24 h period, during the light period, the pCO_2 decreased and the pH increased for each pCO_2 treatment due to net photosynthesis (Fig. 1a,e). During

Table 1. *Pleurochrysis carterae* culture and media chemistry conditions (mean ± SD), including variability experienced during a diel cycle and during a complete growth cycle. Total scale pH (pH_T), temperature, salinity, alkalinity, phosphate, and silicate were measured, and the remaining parameters were calculated using CO2sys software (Pierrot et al. 2006). One-way ANOVAs were performed to identify differences in water chemistry parameters among the 3 treatments (280, 380, or 750 µatm pCO_2); culture parameters and media parameters were considered separately. Treatments with the same superscript letters (uppercase for cultures, lowercase for media) were not significantly different from each other ($p < 0.05$), as determined by Tukey's post hoc test following the ANOVAs. DIC: dissolved inorganic carbon

	pH_T	Temp. (°C)	Salinity (PSU)	Alkalinity (µeq kg^{-1})	Phosphate (µmol kg^{-1})	Silicate (µmol kg^{-1})	DIC (µmol kg^{-1})	pCO_2 (µatm)	$[HCO_3^-]$ (µmol kg^{-1})	$[CO_3^{2-}]$ (µmol kg^{-1})	$[CO_2]$ (µmol kg^{-1})	$\Omega_{calcite}$
280 Culture	8.19 ± 0.10^A	16.6 ± 0.2	32.2 ± 0.4	2056 ± 130	19.1 ± 7.5	20.5 ± 1.9	1763 ± 145	244 ± 69^A	1569 ± 157	186 ± 30^A	8.8 ± 2.5^A	4.52 ± 0.75^A
380 Culture	8.16 ± 0.15^A	16.6 ± 0.3	32.2 ± 0.4	1990 ± 224	16.2 ± 8.5	17.9 ± 4.4	1713 ± 274	265 ± 120^A	1529 ± 293	174 ± 37^A	9.6 ± 4.4^A	4.24 ± 0.89^A
750 Culture	7.85 ± 0.13^B	16.4 ± 0.3	32.2 ± 0.4	1892 ± 349	21.1 ± 12.3	20.4 ± 3.0	1750 ± 362	553 ± 234^B	1638 ± 354	92 ± 18^B	20.1 ± 8.5^B	2.23 ± 0.43^B
280 Media	8.14 ± 0.02^a	17.0 ± 0.1	31.8 ± 0.6	2225 ± 143	26.0 ± 0.5	19.9 ± 0.4	1942 ± 115	303 ± 0.8^a	1751 ± 93	180 ± 22^a	10.9 ± 0.8^a	4.40 ± 0.5^a
380 Media	8.03 ± 0.02^b	17.1 ± 0.1	31.2 ± 0.6	2212 ± 143	26.5 ± 1.9	21.0 ± 0.53	1980 ± 119	402 ± 5^b	1818 ± 102	148 ± 17^{ab}	14.3 ± 0.1^b	3.60 ± 0.4^{ab}
750 Media	7.79 ± 0.01^c	17.1 ± 0.4	31.8 ± 0.5	2228 ± 146	27.5 ± 0.1	21.4 ± 0.7	2095 ± 138	773 ± 32^c	1977 ± 129	90 ± 8^b	27.6 ± 1.3^c	2.20 ± 0.18^b

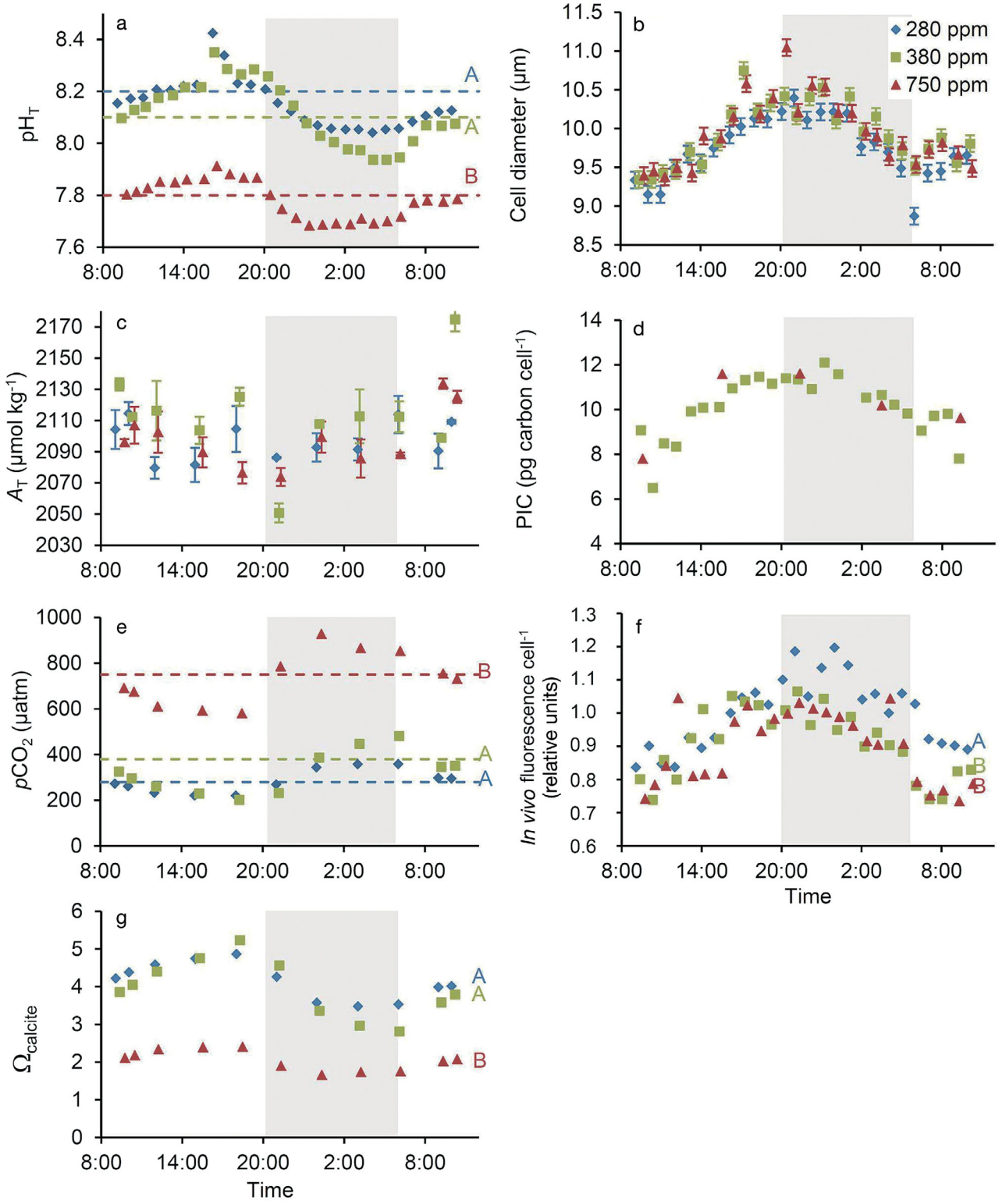

Fig. 1. Culture dynamics of *Pleurochrysis carterae* acclimated to 280, 380, or 750 µatm pCO_2 for >9 generations and measured over 24 h with a 14:10 h light:dark period. (a) pH measured on the total scale (pH_T), with dashed lines representing the target pH for each treatment. (b) Cell diameter. (c) Total alkalinity (A_T). (d) Particulate inorganic carbon (PIC). The 280 µatm treatment is omitted due to inaccurate PIC $cell^{-1}$ measurements. (e) pCO_2, calculated using CO2sys software (Pierrot et al. 2006), with dashed lines representing the target pCO_2 for each treatment. (f) *In vivo* fluorescence normalized to cell abundance. (g) Calcite saturation state ($\Omega_{calcite}$), calculated using CO2sys software (Pierrot et al. 2006). When there were statistical differences among pCO_2 treatments, the results are designated with a letter. Same letters indicate results that were not significantly different from each other. Different letters indicate significant differences. When error bars are shown, they represent ±1 SD. Shaded areas represent the dark period

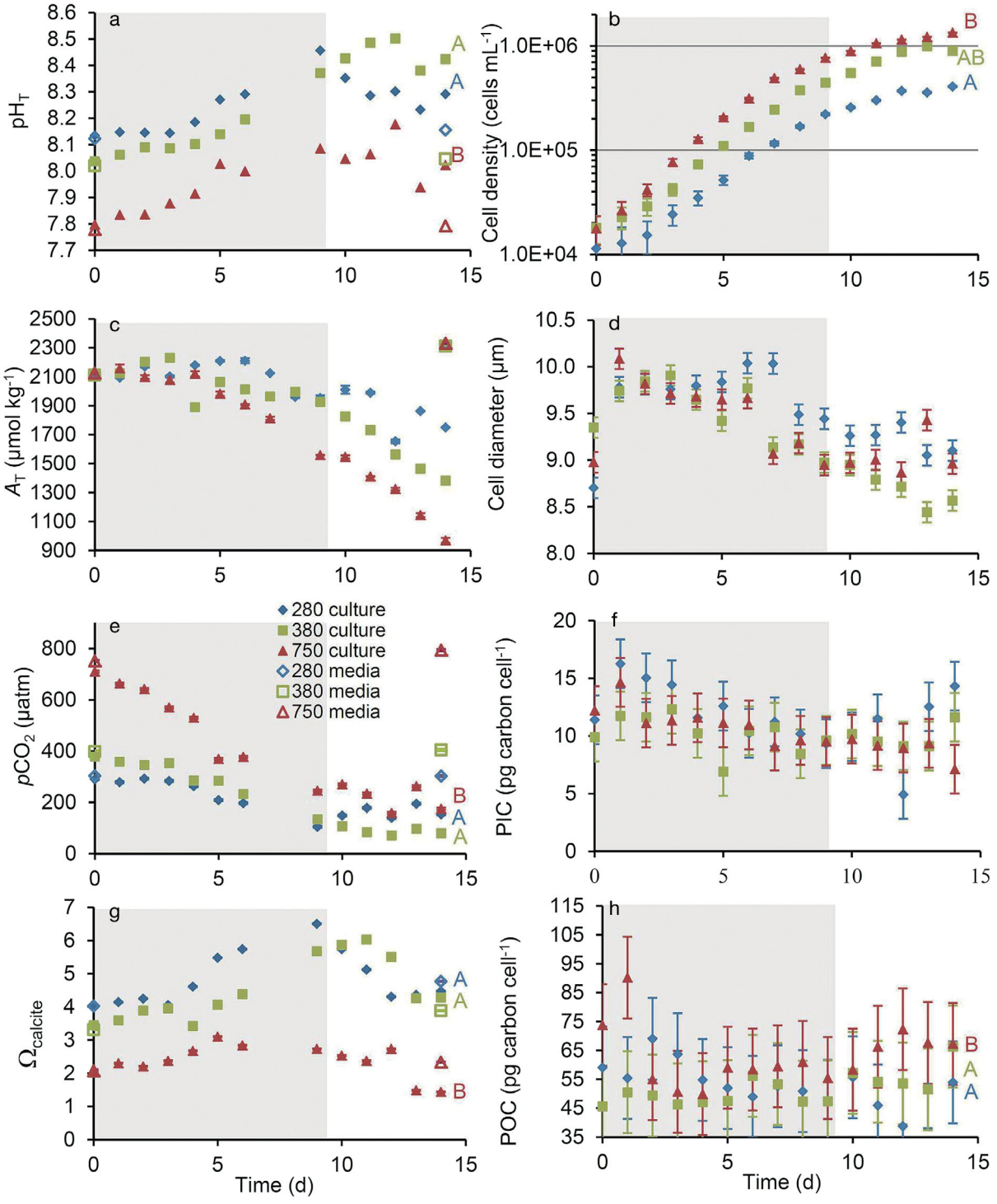

Fig. 2. Culture dynamics of *Pleurochrysis carterae* acclimated to 280, 380, or 750 µatm pCO_2 for >9 generations and measured over one 14 d growth cycle. (a) pH measured on the total scale (pH_T). (b) Cell density. (c) Total alkalinity (A_T). (d) Cell diameter. (e) CO_2 concentration calculated using CO2sys software (Pierrot et al. 2006). (f) Cell particulate inorganic carbon (PIC). (g) Calcite saturation state ($\Omega_{calcite}$), calculated using CO2sys software (Pierrot et al. 2006). (h) Cell particulate organic carbon (POC). Carbonate chemistry measurements of the media for each treatment were made on Days 0 and 14 and represent the chemistry conditions without biological influence. Shaded areas represent the days when the cultures were in exponential growth. When there were statistical differences among pCO_2 treatments, the results are designated with a letter. Same letters indicate results that were not significantly different from each other. Different letters indicate significant differences. Calculations of full carbonate chemistry parameters for Days 7 and 8 of the 14 d growth cycle were not possible due to the pH electrode malfunctioning. When error bars are shown, they represent ±1 SD

Table 2. Results of 1-way ANOVAs of carbonate chemistry of *Pleurochrysis carterae* acclimated to 3 pCO_2 levels for >9 generations (showing which carbonate chemistry variables were significantly related to pCO_2 treatment in each row), including variability experienced during a diel cycle and during a complete growth cycle. pH_T, temperature, salinity, alkalinity, phosphate, and silicate were measured, and the remaining parameters were calculated using CO2sys software (Pierrot et al. 2006). In the degrees of freedom column, the first (second) value is the between-group (within-group) degrees of freedom. **Bolded** p-values represent significant differences among pCO_2 treatments. A_T: total alkalinity, DIC: dissolved inorganic carbon

Variable	SS	df	MS	*F*	p
pH_T	2.84	2,114	1.42	84.39	**<0.001**
Temperature	0.47	2,120	0.23	3.14	**0.047**
Salinity	0.05	2,120	0.03	0.19	0.828
A_T	3.45×10^5	2,74	1.73×10^5	2.77	0.069
Phosphate	376.51	2,89	188.25	2.03	0.137
Silicate	26.47	2,15	13.24	1.24	0.319
DIC	32033.89	2,69	1.60×10^4	0.21	0.810
pCO_2	1.43×10^6	2,69	7.15×10^5	28.89	**<0.001**
$[HCO_3^-]$	1.46×10^5	2,69	7.31×10^4	0.93	0.400
$[CO_3^{2-}]$	1.27×10^5	2,69	6.36×10^4	74.01	**<0.001**
$[CO_2]$	1894.85	2,69	947.42	29.12	**<0.001**
$\Omega_{calcite}$	75.35	2,69	37.67	74.43	**<0.001**

the dark period, the pCO_2 increased and the pH decreased for each pCO_2 treatment due to net respiration. For both pH and pCO_2, the variability was centered around the target level set for each treatment (Fig. 1a,e). These diel changes due to photosynthesis and respiration resulted in $\Omega_{calcite}$ conditions that increased during the light period and decreased at night for all treatments, with a significant difference between the 750 µatm treatment and the 280 and 380 µatm treatments (Tables 1 & 2, Fig. 1g). Cell diameter, cellular PIC, and fluorescence all increased during the light period and decreased during the dark period, with no significant differences among treatments for cell diameter and cellular PIC (Fig. 1, Table 3). Fluorescence normalized to cell density was significantly higher in the 280 µatm treatment than in the 380 and 750 µatm treatments (Fig. 1f, Table 3).

During a 14 d growth cycle, with the exponential growth phase lasting from Days 0–9 (Fig. 2b), pH steadily increased throughout the exponential stage, at which point pH stabilized and in 1 case (280 µatm) slightly declined, although not significantly (Fig. 2a). The growth rate of the cells during log-phase growth was not statistically different for the different pCO_2 treatments (0.53 ± 0.13 d^{-1}). During exponential growth, pCO_2 declined in each treatment and then remained relatively constant and low during stationary phase (Fig. 2e). These changes correspond to the increasing uptake of CO_2 during photosynthesis by an exponentially growing biomass of algae. During the 14 d growth cycle, A_T declined with time in each treatment (Fig. 2c) as a result of bicarbonate lost to calcification and due to assimilation of NO_3^- and PO_4^{3-} by the algae (Fig. 3) (Wolf-

Table 3. Results of 1-way ANOVAs of cell dynamics of *Pleurochrysis carterae* acclimated to 3 pCO_2 levels for >9 generations and measured hourly over a 24 h period or daily over a 14 d period. **Bolded** p-values represent significant differences among pCO_2 treatments. PIC (POC): particulate inorganic (organic) carbon

Experiment	Variable	Error source	SS	df	MS	*F*	p
24 h cycle	Cell abundance	pCO_2 treatment	9.36×10^9	2	4.68×10^9	54.20	**<0.001**
		Error	6.48×10^9	75	8.64×10^7		
	Cell diameter	pCO_2 treatment	0.63	2	0.31	1.85	0.163
		Error	12.65	75	0.17		
	PIC $cell^{-1}$	pCO_2 treatment	0.90	1	0.90	0.16724	0.686
		Error	150.19	28	5.36		
	Fluorescence $cell^{-1}$	pCO_2 treatment	0.00	2	0.00	6.7471	**0.002**
		Error	0.00	75	0.00		
14 d cycle	Cell density	pCO_2 treatment	1.16×10^{12}	2	5.79×10^{11}	4.57	**0.016**
		Error	5.32×10^{12}	42	1.27×10^{11}		
	Cell diameter	pCO_2 treatment	0.65	2	0.32	1.77	0.182
		Error	7.69	42	0.18		
	PIC $cell^{-1}$	pCO_2 treatment	21.92	2	10.96	2.57	0.089
		Error	179.34	42	4.27		
	POC $cell^{-1}$	pCO_2 treatment	1129.53	2	564.76	8.88	**<0.001**
		Error	2669.99	42	63.57		

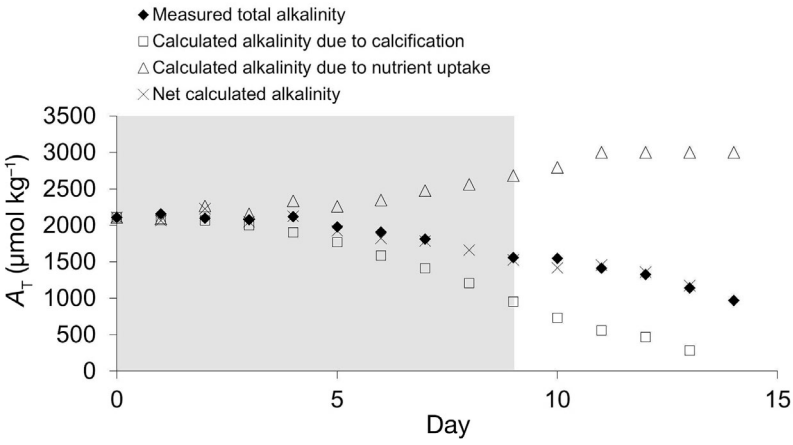

Fig. 3. Measured and calculated total alkalinity (A_T) of a *Pleurochrysis carterae* culture acclimated to 750 µatm pCO_2 for >9 generations and measured over one 14 d growth cycle. Change in A_T as a result of calcification was calculated based on daily particulate inorganic carbon (PIC) measurements. Change in A_T as a result of nutrient assimilation was calculated on daily [NO_3^-] and [PO_4^{3-}] measurements. Net calculated alkalinity represents the change in alkalinity reflecting both calcification and nutrient assimilation. The PIC measurement on Day 14 was an outlier and was excluded from calculations. The shaded area represents the days when the culture was in exponential growth

Gladrow et al. 2007). This changing chemistry resulted in $\Omega_{calcite}$ values that increased for each treatment during the exponential growth phase (Fig. 2g). Despite variable conditions, the 280 and 380 µatm treatments remained significantly different from the 750 µatm treatment with respect to pH_T, pCO_2, and $\Omega_{calcite}$ (Fig. 2, Tables 1 & 2).

Pleurochrysis carterae cell diameter began at low values, characteristic of early stationary phase cells, quickly increased, and then remained relatively constant until Day 7, then decreased over the remaining 14 d growth cycle, as did PIC cell^{-1}, with no significant differences among treatments (Fig. 2d,f, Table 3). POC cell^{-1} did not follow an obvious pattern during the growth cycle, although the 750 µatm pCO_2 treatment had significantly higher POC cell^{-1} than the 280 and 380 µatm treatments (Fig. 2h, Table 3).

Light-dependency of calcification

Coccoliths of *P. carterae* were almost completely dissolved by 2 min exposure to HCl, followed by neutralization with NaOH (Fig. 4a,b). Sufficient coccoliths reformed after 24 h incubation in either light (Fig. 4c) or dark conditions (Fig. 4d) to reliably count the number of coccoliths formed cell^{-1}. Coccolith formation (following de-calcifying with HCl) was used as a proxy for calcification and was significantly faster in cells acclimated to 380 and 750 µatm pCO_2 than in cells acclimated to 280 µatm pCO_2 (Fig. 5, Table 4). Furthermore, coccolith formation was significantly faster in cells incubated in light conditions relative to cells incubated in dark conditions (Fig. 5, Table 4), indicating some, but not complete, light-dependency of calcification. There was no significant interaction between pCO_2 treatment and light conditions during incubation (Table 4). Some coccoliths remained after the de-calcifying treatment with HCl and neutralization with NaOH (Fig. 4b). Moreover, few coccoliths formed per cell following 24 h dark incubation (Fig. 4d). A comparison of the average coccoliths cell^{-1} after de-calcifying and neutralization with the average cellular coccoliths following 24 h dark incubation demonstrated that with the exception of the 280 µatm treatment, there were significantly more coccoliths cell^{-1} following the 24 h dark incubation (2-way ANOVA, F_1 = 18.13, p = 0.005) than following the de-calcifying treatment, supporting the conclusion that there was a significant amount of calcification during the 24 h dark incubation.

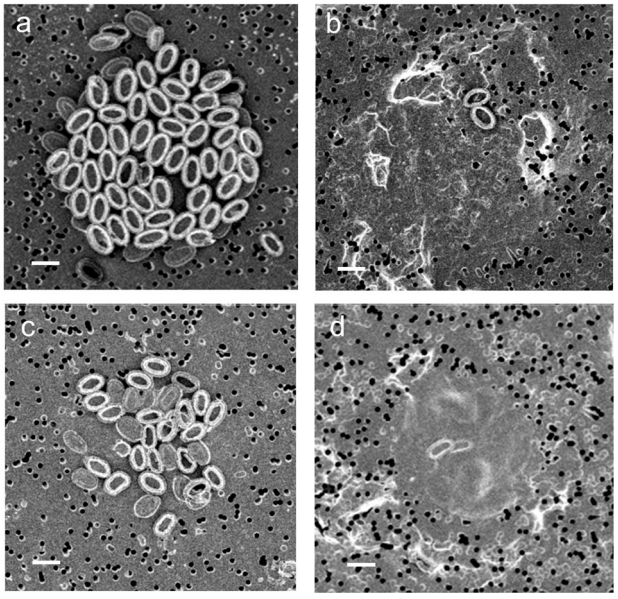

Fig. 4. Scanning electron micrographs of various *Pleurochrysis carterae* cells. (a) Cell prior to de-calcification and (b) cell after de-calcification by acidification to pH = 5.5 with HCl. (c, d) Previously de-calcified cells at the end of the 24 h incubation in (c) light or (d) dark conditions. Scale bars = 2 µm

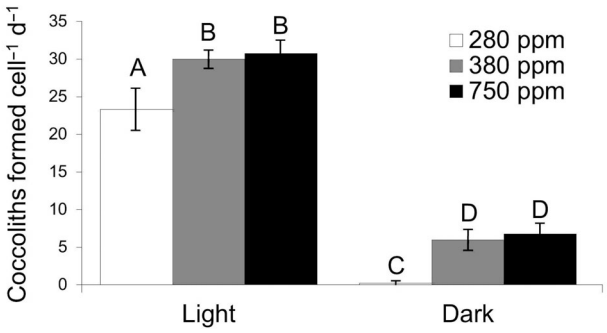

Fig. 5. Calcification of *Pleurochrysis carterae* acclimated to 3 pCO_2 treatments for >9 generations and grown for 24 h in either light or dark conditions. Calcification was approximated by the number of coccoliths formed cell^{-1} during the 24 h incubation, following complete de-calcification. Different letters indicate significant differences among pCO_2 treatments. Error bars represent 1 SD

Table 4. Results of 2-way ANOVA of coccolith formation by *Pleurochrysis carterae* acclimated to 3 pCO_2 levels for >9 generations, de-calcified by acidification with HCl, and subsequent 24 h incubation in either light or dark conditions. **Bolded** p-values represent significant differences among treatments

Error source	SS	df	MS	*F*	p
pCO_2 treatment	176.73	2	88.37	31.67	**<0.001**
Light treatment	2532.55	1	2532.35	907.47	**<0.001**
pCO_2 × Light	0.87	2	0.44	0.16	0.86
Error	33.49	12	2.79		

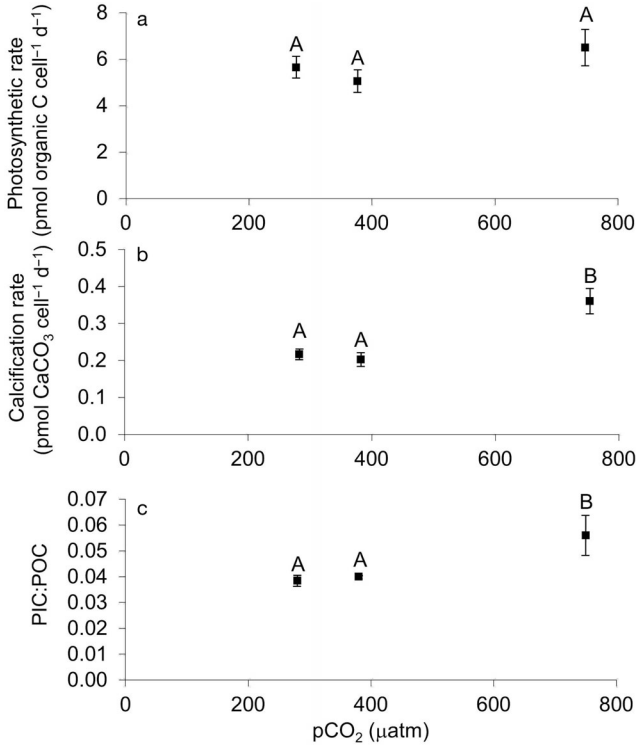

Fig. 6. (a) Photosynthetic and (b) calcification rates and (c) particulate inorganic carbon to particulate organic carbon production ratios (PIC:POC), expressed as the ratio of photosynthetic to calcification rates, of *Pleurochrysis carterae* acclimated to 3 pCO_2 levels for >9 generations. Values represent mean ± SD. Rates were measured by the ^{14}C microdiffusion technique and were normalized to cell density. Different letters indicate significant differences among pCO_2 treatments

Photosynthetic and calcification rates

P_{24} and C_{24} rates measured using the ^{14}C-microdiffusion technique (see Eqs. 2 & 3) showed increased rates in the phytoplankton acclimated to 750 µatm pCO_2, although this increase was only significant for C_{24} (Fig. 6, Table 5). Based on an estimate of 0.35 × 10^{-14} mol Ca per *P. carterae* coccolith (van der Wal et al. 1987), C_{24} correspond to coccolith formation rates of 62, 57, and 103 coccoliths cell^{-1} d^{-1} for cells acclimated to 280, 380, and 750 µatm pCO_2, respectively, with the obvious caveat that these rates are based on 3 h incubations, with 24 h rates approximated from Eq. (2). The PIC:POC production ratio was significantly higher for cells acclimated to 750 µatm pCO_2 than for cells acclimated to 280 or 380 µatm pCO_2 (Fig. 6c). This increased ratio was primarily driven by the increase in C_{24} for cells acclimated to 750 µatm pCO_2.

Table 5. Results of 1-way ANOVAs of photosynthetic and calcification rates (P_{24} and C_{24}, respectively) and particulate inorganic carbon to particulate organic carbon production ratios (PIC:POC) of *Pleurochrysis carterae* acclimated to 3 pCO_2 levels for >9 generations. **Bolded** p-values represent significant differences among pCO_2 treatments

Variable	Error source	SS	df	MS	*F*	p
Photosynthetic rate	pCO_2 treatment	3.16	2	1.58	4.4	0.067
	Error	2.16	6	0.36		
Calcification rate	pCO_2 treatment	0.046	2	0.023	37.98	**<0.001**
	Error	0.0037	6	0.0006		
PIC:POC	pCO_2 treatment	0.0006	2	0.0003	12.53	**0.007**
	Error	0.0001	6	0.00002		

DISCUSSION

Culture chemistry and cellular dynamics

The field of OA research is rapidly advancing, with new knowledge bringing new recommendations for manipulation experiments. For exam-

ple, in the European Project on Ocean Acidification (EPOCA) Guide to best practices for OA research and data reporting, LaRoche et al. (2010, p. 89) recommended dilute batch culturing of phytoplankton due to 'the need to keep the carbonate chemistry as constant as possible.' However, just 5 yr later, with more knowledge about the extremely variable carbonate chemistry in coastal waters (Feely et al. 2010, Wallace et al. 2014, Baumann et al. 2015), calls are being made for experimental manipulations replicating the natural variability of the organisms' natural environment (Gledhill et al. 2015, Boyd et al. 2016). Boyd et al. (2016) pointed out that oceanic organisms, and particularly coastal organisms, are faced with environmental heterogeneity that varies over time scales ranging from diel (photosynthetic- and respiration-driven) to decadal (i.e. the El Nino-Southern Oscillation). The majority of OA perturbation experiments have used stable treatments, overlooking the natural variability that species encounter. However, Cornwall et al. (2013) found that response of calcifying macroalgae to OA varied based on whether the pH treatments were stable or variable around a mean pH level. Our carbonate chemistry manipulation method of controlling only the pCO_2 of the incoming gas allowed the carbonate chemistry of the culture to vary gradually on diel (Fig. 1) and fortnightly time scales (Fig. 2), due to changes in biological activity of the cultures. The range of the diel variability (ca. ±0.2 pH units around the target mean) in our cultures was similar to the mid-range pH variability seen in a temperate tidal salt marsh (Baumann et al. 2015). The increase in pH seen over a 14 d growth cycle (Fig. 2a) is similar to the pH increases that have been observed for natural phytoplankton blooms over time scales of 20–25 d (Brussaard et al. 1996, Hinga 2002). Therefore, our cultures were exposed to pCO_2 conditions that fluctuated around mean treatment levels that represent future pCO_2 conditions, based on atmospheric pCO_2 changes. The fluctuations around these mean treatment levels more realistically represent the environmental heterogeneity that coastal species, such as *Pleurochrysis carterae*, experience on different time scales. Because the range of conditions experienced by the 280 (preindustrial) and 380 µatm pCO_2 treatments (near-ambient) were generally not significantly different from each other, coastal species may not yet be experiencing carbonate chemistry conditions that are outside of the range they experienced prior to the industrial revolution. We caution that these experiments were performed in 2013, the average annual pCO_2 at Mauna Loa was 396.5 ppmv, and for the last full year of data in 2017, the pCO_2 was 406.5 ppmv, both of which have surpassed the level we used as our near-ambient concentration (380 µatm pCO_2) (Dlugokencky & Tans 2018, Le Quéré et al. 2018). However, it should be noted that previous work considering pre-industrial and ambient pCO_2 treatments with quasi-stable conditions has shown significant biological impacts between these treatment levels (Talmage & Gobler 2010).

A_T decreased in each pCO_2 treatment throughout the 14 d growth cycle. However, during the exponential phase, $\Omega_{calcite}$ steadily increased, indicating that during this stage, the increasing pH had a stronger impact on $\Omega_{calcite}$ (by shifting the DIC equilibrium) than did the decreasing A_T associated with calcification. The decrease in alkalinity can be nearly entirely explained by the measured nutrient uptake and measured increase in PIC, the latter representing net calcification (Fig. 3). While the nitrate ion itself does not contribute to alkalinity, the process of nitrate uptake by phytoplankton must be accompanied by cotransport of a positive ion, generally assumed to be H^+ (Wolf-Gladrow et al. 2007), which increases alkalinity by 1 µequivalent per µmol nitrate assimilated. Similarly, cotransport of H^+ with phosphate also increases alkalinity by 1 µmol kg^{-1} per µmol phosphate assimilated (Wolf-Gladrow et al. 2007). The coccolithophore *Emiliania huxleyi* uses bicarbonate as the inorganic carbon source for calcification (Paasche 1964, Buitenhuis et al. 2003, Bach et al. 2013), and evidence indicates that *P. carterae* also uses bicarbonate, although some low calcifying strains may be able to use CO_2 as the carbon source for calcification (Israel & González 1996). The stoichiometry of calcification generally follows that, for each mole of $CaCO_3$ produced, alkalinity is reduced by 2 equivalents from the loss of 2 bicarbonate ions. There are some exceptions to this, however, as a function of growth rate (Balch et al. 1996).

Nonetheless, for our 14 d growth cycle observational period, the calculated sum of the nitrate uptake effect and calcification effect, based on daily measured nutrient and PIC concentrations, is in close agreement with the measured alkalinity (Fig. 3). Such a decrease in alkalinity as we observed here has been observed during coccolithophore blooms (Balch et al. 2016).

Cell size variability over a diel cycle show similar patterns to those observed by van der Wal et al. (1987), with increasing cell diameter during the light cycle and decreasing cell diameter during the dark cycle. This increase in cell size during the light cycle is attributed to preparation for cell division (van der Wal et al. 1987), which takes place mainly during the

dark period. Our data showing an increase in the relative fluorescence normalized to cell density during the light cycle and a decrease during the dark cycle (Fig. 1f) support this conclusion. The increase in cellular PIC during the light cycle and decrease during the dark cycle is explained as coccolith production stimulated by an increase in the cell surface area as cells prepare for division during the dark period (van der Wal et al. 1987). The decrease in cellular PIC during the dark period may also represent partial dissolution of the coccoliths due to respiratory CO_2 production reducing the pH near the cell surface, such that the chemistry of the microenvironment around the cell surface may be substantially different than that of the bulk culture (Flynn et al. 2012), which remained supersaturated with respect to calcite in all pCO_2 treatments, even during the dark period. Unfortunately, we did not have any SEM images that might have provided direct evidence of malformed coccoliths to explain the dark decrease in PIC.

Light-dependency of calcification

The light-dependency of *P. carterae* calcification has been investigated by others, with results indicating that the dark calcification rate of *P. carterae* is dependent on the length of the dark exposure. Early work initially indicated that coccolith formation is light-dependent (Dorigan & Wilbur 1973), with little to no calcification during dark periods lasting up to 7 d. However, subsequent work showed that the rates of calcification were similar during the light and dark periods of an alternating 16:8 h light:dark incubation, but calcification significantly decreased by 24 h in continuous darkness, and eventually ceased (van der Wal et al. 1987). Similarly, Moheimani & Borowiztka (2011) found that *P. carterae* were able to calcify during the latter half of a 12 h dark period of a 12:12 h light:dark incubation, although the concentration of coccoliths initially decreased during the dark period, which the authors interpreted as dissolution due to respiratory CO_2.

One other group investigated the impact of pCO_2 on dark calcification in *P. carterae* and found negative net calcification rates during 7 d dark incubations, indicating calcite dissolution at both 390 and 1200 µatm pCO_2. However, they found a significantly more negative net calcification rate at 1200 relative to 390 µatm pCO_2, despite both treatments being supersaturated with respect to calcite (Casareto et al. 2009). It should be noted that in the work of Carsareto et al (2009) *P. carterae* was inoculated into unfiltered seawater samples, which may have exposed the algae to greater rates of community respiration than an axenic algal culture, potentially increasing respiratory CO_2-driven dissolution, thus complicating the interpretation. Because a 7 d dark exposure exceeds the length of time in which calcification ceases in the dark (van der Wal et al. 1987), measuring net calcification over this time period may have missed observations of dark calcification early-on during the dark period. Furthermore, significant differences between our experimental design and that of Casareto et al. (2009) likely contribute to the different results regarding the impact of pCO_2 on the dark calcification rate of *P. carterae*. Bach et al. (2015) demonstrated that simply the differences in the light intensity and temperature experienced by the same strain of coccolithophore can produce different responses to similar pCO_2 ranges.

Our work further supports the observations of others that *P. carterae* has the ability to calcify under short-term dark conditions, although we found reduced dark calcification rates relative to light calcification rates (dark calcification = 0.9, 19.8, and 21.9% of light calcification for 280, 380, and 750 µatm pCO_2, respectively; Fig. 5). This reduction in calcification rate in dark conditions was not seen by van der Wal et al. (1987) and may have been influenced by the timing of the start of our 24 h incubations. For this experiment, our replicates were de-calcified by acidification just prior to the end of the 10 h dark period of the 14:10 h light:dark cycle. Once the cultures were neutralized to restore the original pH, the 24 h incubation period started. Therefore, the cells in the dark treatment were actually in the dark for 34 continuous hours by the end of the experiment, thus their energetic reserves would have been severely limited. Van der Wal et al. (1987) found that the rate of calcification decreased significantly with time of dark incubation, with significant reduction after 24 h of dark incubation. As with our results, this reduction is thought to be due to depletion of energy reserves in the absence of photosynthesis.

Regardless of light conditions, the calcification rates of algae acclimated to 380 and 750 µatm were significantly greater than those of algae acclimated to 280 µatm pCO_2. Moreover, the effect of pCO_2 on calcification rates was the same during both light and dark incubations (despite any stress associated with the de-plating of the cells in the light–dark experiment). Thus, the hypothesis that calcification at high pCO_2 (with lower $\Omega_{calcite}$) may be energy-limited in the dark is not supported (Monteiro et al. 2016). Instead, at CO_2 conditions that are elevated relative

to pre-industrial conditions, calcification rates increased significantly.

Photosynthetic and calcification rates

Using the highly-sensitive ^{14}C-microdiffusion technique, we found no significant impact of pCO_2 on *P. carterae* photosynthetic rate (Fig. 6a), but a significant increase in both the calcification rate and PIC:POC production ratio with increasing pCO_2 (Fig. 6b,c). Note that when the calcification rate was converted to the equivalent number of coccoliths produced per day, this translated to coccolith formation rates of 62, 57, and 103 coccoliths cell^{-1} d^{-1} for cells acclimated to 280, 380, and 750 µatm pCO_2, respectively. This is reasonable compared to values of 100–200 coccoliths cell^{-1} for *P. carterae*, reported by van der Wal et al. (1987).

In addition, we did not find a significant impact of pCO_2 on *P. carterae* growth rate (which averaged 0.53 ± 0.13 d^{-1} as noted in the Results). In combination, the photosynthetic and growth rate results indicate that *P. carterae* is not carbon-limited at current atmospheric CO_2 conditions and does not benefit photosynthetically from increased atmospheric CO_2 levels (CO_2 fertilization). Similarly, a meta-analysis of 24 experiments found no significant impact of increased CO_2 on *E. huxleyi* photosynthetic rates, indicating that this species is also not currently facing carbon-limitation (Meyer & Riebesell 2015; see also Rivero-Calle et al. 2015). However, *Gephyrocapsa oceanica* was found to have significantly increased photosynthetic rates at both 380 and 1000 µatm, relative to 280 µatm (Meyer & Riebesell 2015), which may indicate that there are species-specific differences among coccolithophores with regard to current CO_2-saturation levels for carbon fixation.

The theory that calcification becomes more energetically costly at lower saturation states has been supported for multiple invertebrate taxa (Drenkard et al. 2013, Waldbusser et al. 2013, Houlbrèque et al. 2015), but is perhaps overly simplistic for autotrophic organisms, as the corresponding increase in CO_2 may be beneficial for photosynthesis, indirectly supplying more energy for calcification. Nonetheless, it has been hypothesized that the majority of calcifying organisms will be negatively affected by OA (Orr et al. 2005). Indeed, some of the first work regarding the impact of OA on coccolithophore calcification showed a decline in calcification rates of *E. huxleyi* and *G. oceanica* with increasing pCO_2 (Riebesell et al. 2000). However, other work has shown an increase in *E. huxleyi* calcification rates with increasing pCO_2 (Iglesias-Rodriguez et al. 2008), and still others have shown *E. huxleyi* to have optimum-shaped curves with an initial increase in cellular calcification rate with increasing pCO_2, from 200 to 600 µatm pCO_2 followed by a decrease in cellular calcification rate with further increasing pCO_2 up to ~900 µatm pCO_2 (Langer et al. 2009, Hoppe et al. 2011). Ultimately, based on 24 experiments, *E. huxleyi* exhibits a significant decline in calcification rates at 780 and 1000, relative to 280 µatm (Meyer & Riebesell 2015).

With regard to *P. carterae*, it is difficult to compare the increased calcification rate that we observed for algae acclimated to 750 µatm pCO_2 with existing literature because the 2 existing studies considering the effects of CO_2 on *P. carterae* report bulk culture net calcification rates, not per cell net calcification rates. Moheimani & Borowitzka (2011) found decreased bulk culture calcite production at pCO_2 levels ranging from 835–1350 µatm, relative to calcite production at 461–603 µatm pCO_2. However, both treatments represent an increase in bulk culture calcite production relative to cultures where the pH was uncontrolled and pCO_2 ranged from 3–267 µatm. Moreover, Casareto et al. (2009) found a non-significant increase in the net calcification rate of *P. carterae* cultures grown for 7 d at 1200 µatm, relative to ambient pCO_2 with no conclusions possible on cellular rates.

Application of the substrate-inhibitor concept

Bach et al. (2015) provided a substrate-inhibitor concept describing the dependence of calcification rates on carbonate chemistry speciation. This concept incorporates the ideas that coccolithophore calcification rates increase with increasing HCO_3^-, which acts as a primary substrate for calcification, and with increasing CO_2, which can limit photosynthesis, thereby indirectly affecting calcification by limiting the supply of energy necessary for calcification. Furthermore, calcification can be inhibited by increased proton concentrations (Bach et al. 2015). When applied here, it appears that calcification rates may be enhanced by the increased availability of bicarbonate ions in the 380 and 750 µatm pCO_2 treatments, but not yet inhibited by the increased H^+ concentrations in these 2 treatments, relative to the 280 µatm treatment. However, due to the variable carbonate chemistry conditions of our cultures, which fluctuate around a mean target value, the

bicarbonate concentrations were not significantly different among any of the treatments (Table 1). Similarly, pH was not significantly different between the 280 and 380 µatm treatments, although it was significantly lower (higher [H^+]) in the 750 µatm treatment. It may be that high variability of the culture conditions, measured on diel and 2 wk time scales, obscured a baseline shift in carbonate chemistry conditions. Indeed, although not significant, the 380 µatm treatment attained lower pH and $\Omega_{calcite}$ conditions towards the end of the dark period than did the 280 µatm treatment (Fig. 1a,g). Similarly, throughout the 9 d of exponential growth during the 14 d growth cycle, the 380 µatm treatment had consistently lower pH and $\Omega_{calcite}$ conditions than the 280 µatm treatment.

The observed increase in *P. carterae* calcification rate at 750 µatm also fits into the substrate-inhibitor concept presented by Bach et al. (2015). This model simulates the optimum curves similar to those observed experimentally by Langer et al. (2009) and Hoppe et al. (2011). While it would have been ideal to model the *P. carterae* data presented in this study in the context of the Bach et al. (2015) substrate-inhibitor concept, we have too few data points to model. However, based on the relative surface area to volume ratio and PIC:POC ratio of *P. carterae*, we can attempt to estimate where *P. carterae* would fit into this model based on relative calcification rates. The actual calcification optima and sensitivities for any species will depend on many factors regarding the culture conditions, including temperature, light levels, and nutrient levels (Bach et al. 2015). Larger species (*Calcidiscus leptoporus* and *Coccolithus pelagicus*, coccosphere diameter 14.7 and 15.3 µm, respectively) have lower surface area to volume ratios and require a higher HCO_3^- concentration to saturate HCO_3^- flux into the cell, resulting in calcification optima at higher pCO_2 levels. The coccosphere of *P. carterae* (NCMA strain 645) is approximately 9–10 µm (Figs. 1b & 2d), which is in the middle of the coccosphere range for the 4 species modeled by Bach et al. (2015). As a result, *P. carterae* should have a relative calcification optimum that falls at a pCO_2 level between that of *G. oceanica* and *C. pelagicus*. In their model, *G. oceanica*, *C. pelagicus*, and *C. leptoporus* have significantly greater sensitivities to increased pCO_2 beyond their calcification optima than does *E. huxleyi* (Bach et al. 2015). This is attributed to the PIC:POC ratios for these 3 species being approximately twice that of *E. huxleyi*. The higher the calcification rate is, relative to the photosynthetic rate, the more H^+ that must be transported out of the cell to prevent cytosol acidification. As seawater pCO_2 levels and H^+ concentrations increase, this transport will become more difficult. The PIC:POC ratio measured for *P. carterae* in this study ranges from 0.04 to 0.055, which is a small fraction of the PIC:POC ratio reported for *E. huxleyi* (1.2) by Bach et al. (2015). As such, *P. carterae* should be less sensitive to high pCO_2 conditions than *E. huxleyi*, which was the least sensitive of the 4 species modeled. While the relative calcification optimum for *P. carterae*, estimated from the ratio of cell surface area to volume and PIC:POC ratios (Bach et al. 2015)(Fig. 3), lies at a pCO_2 level lower than that observed in the present study, the actual pCO_2 level of the *P. carterae* calcification optimum will be determined by specific culture conditions (Bach et al. 2015). Aside from this substrate-inhibitor concept, which suggests a calcification optimum based on carbonate chemistry speciation, an increase in calcification with increasing pCO_2 may provide protection from predators. The modeling work of Irie et al. (2010) suggests that as the ocean pH decreases, bloom-forming coccolithophores will benefit more from having a more heavily calcified exoskeleton (coccoliths) to reduce instantaneous mortality than from having an accelerated cell cycle.

An increase in calcification in the estuarine *P. carterae* and similar coccolithophores at future pCO_2 levels could have a positive feedback on acidification of coastal waters during bloom conditions, as calcification both decreases alkalinity and increases DIC. However, because *P. carterae* has such low PIC:POC ratio, during exponential growth, the photosynthetic drawdown of CO_2 has a greater impact on $\Omega_{calcite}$ than the reduction in alkalinity and increase in DIC associated with calcification (Fig. 2). Furthermore, in estuarine waters, upon deposition into the shallow, low $\Omega_{calcite}$-sediments (Green & Aller 1998, Waldbusser & Salisbury 2014), *P. carterae* coccoliths will likely dissolve relatively quickly, increasing alkalinity and decreasing DIC, with no net pumping of alkalinity from the surface to the benthic environment. With algal blooms increasing in the future due to increased nutrient pollution (Alam & Dutta 2013), these biogeochemical processes may exacerbate coastal carbonate chemistry variability, creating more extreme unfavorable conditions for commercially important coastal heterotrophs, such as shellfish. The effects that *P. carterae* have on seawater chemistry during photosynthesis and calcification seem unlikely to mitigate coastal OA.

Overall, our work supports the unifying 'substrate-inhibitor' concept of Bach et al. (2015) describing

variable responses to OA among coccolithophore species and strains that seem contradictory at first. Calcification rates can be enhanced by increased availability of bicarbonate as a result of OA; however, decreases in calcification can occur due to inhibitory [H^+], resulting in optimum calcification rates at pCO_2 levels that vary by species. These results indicate that with further species-specific information including coccosphere size and PIC:POC ratios, as well as species-specific responses to varying light, temperature, and nutrients, we may be able to predict the pCO_2 level at which a given coccolithophore species will show its optimum calcification rate.

Data archive. Datasets from this work are available through the Biological and Chemical Oceanography Data Management Office (BCO-DMO) at www.bco-dmo.org/project/514415.

Acknowledgements. This work was supported by NOAA Award NA11OAR4310055 awarded to David M. Fields (Bigelow Laboratory for Ocean Sciences) and W.M.B. and by NSF Bio-OCE Grant 1220068 awarded to David M. Fields and W.M.B., and including postdoctoral support for M.M.W. We thank Emily Lyczkowski for experimental assistance and Rosaline Campbell for performing alkalinity titrations. We also thank Ashley Poehls and Steve Shema for help with preliminary method development and experimental design. Three anonymous reviewers kindly reviewed an earlier version of the manuscript and provided insightful comments.

LITERATURE CITED

Alam MJ, Dutta D (2013) Predicting climate change impact on nutrient pollution in waterways: a case study in the upper catchment of the Latrobe River, Australia. Ecohydrology 6:73–82

Andersen RA (ed) (2005) Algal culturing techniques. Elsevier, San Diego, CA

Bach LT, Mackinder LCM, Schulz KG, Wheeler G, Schroeder DC, Brownlee C, Riebesell U (2013) Dissecting the impact of CO_2 and pH on the mechanisms of photosynthesis and calcification in the coccolithophore *Emiliania huxleyi*. New Phytol 199:121–134

Bach LT, Riebesell U, Gutowska MA, Federwisch L, Schulz KG (2015) A unifying concept of coccolithophore sensitivity to changing carbonate chemistry embedded in an ecological framework. Prog Oceanogr 135:125–138

Balch WM, Fritz J, Fernandez E (1996) Decoupling of calcification and photosynthesis in the coccolithophore *Emiliania huxleyi* under steady-state light-limited growth. Mar Ecol Prog Ser 142:87–97

Balch WM, Drapeau D, Fritz J (2000) Monsoonal forcing of calcification in the Arabian Sea. Deep Sea Res II 47: 1301–1337

Balch WM, Bates NR, Lam PJ, Twining BS and others (2016) Factors regulating the Great Calcite Belt in the Southern Ocean and its biogeochemical significance. Global Biogeochem Cycles 30:1124–1144

Barcelos e Ramos J, Müller MN, Riebesell U (2010) Short-term response of the coccolithophore *Emiliania huxleyi* to an abrupt change in seawater carbon dioxide concentrations. Biogeosciences 7:177–186

Baumann H, Wallace RB, Tagliaferri T, Gobler CJ (2015) Large natural pH, CO_2 and O_2 fluctuations in a temperate tidal salt marsh on diel, seasonal, and interannual time scales. Estuaries Coasts 38:220–231

Boyd PW, Cornwall CE, Davison A, Doney SC and others (2016) Biological responses to environmental heterogeneity under future ocean conditions. Glob Change Biol 22:2633–2650

Brownlee C, Taylor AH (2004) Calcification in coccolithophores: a cellular perspective. In: Thierstein HR, Young JR (eds) Coccolithophores — from molecular processes to global impact. Springer, New York, NY, p 31–49

Brownlee C, Nimer N, Dong LF, Merritt MJ (1994) Cellular regulation during calcification in *Emiliania huxleyi*. In: Green JC, Leadbeater BSC (eds) The haptophyte algae, Vol 51. Claredon Press, Oxford, p 133–148

Brussaard CPD, Gast GJ, van Duyl FC, Riegman R (1996) Impact of phytoplankton bloom magnitude on a pelagic microbial food web. Mar Ecol Prog Ser 144:211–221

Buitenhuis ET, Timmermans KR, De Baar HJW (2003) Zinc-bicarbonate colimitation of *Emiliania huxleyi*. Limnol Oceanogr 48:1575–1582

Cai WJ, Hu X, Huang WJ, Murrell MC and others (2011) Acidification of subsurface coastal waters enhanced by eutrophication. Nat Geosci 4:766–770

Caldeira K, Wickett ME (2003) Oceanography: anthropogenic carbon and ocean pH. Nature 425:365

Casareto BE, Niraula MP, Fujimura H, Suzuki Y (2009) Effects of carbon dioxide on the coccolithophorid *Pleurochrysis carterae* in incubation experiments. Aquat Biol 7:59–70

Clayton TD, Byrne RH (1993) Spectrophotometric seawater pH measurements: total hydrogen ion concentration scale calibration of *m*-cresol purple and at-sea results. Deep Sea Res I 40:2115–2129

Cornwall CE, Hepburn CD, McGraw CM, Currie KI and others (2013) Diurnal fluctuations in seawater pH influence the response of a calcifying macroalga to ocean acidification. Proc R Soc B 280:20132201

de Vrind-de Jong EW, de Vrind JPM (1997) Algal deposition of carbonates and silicates. Rev Mineral 35:267–307

de Vrind-de Jong EW, Borman AH, Thierry R, Westbroek P, Grüter M, Kamerling JP (1986) Calcification in the coccolithophorids *Emiliania huxleyi* and *Pleurochrysis carterae* II. Biochemical aspects. In: Leadbeater BSC, Riding R (eds) Biomineralization in lower plants and animals, Spec Vol 30. Systematics Association, Oxford, p 205–218

Dickson AG (1990) Standard potential of the reaction: $AgCl_{(s)} + 12H_{2(g)} = Ag_{(s)} + HCl_{(aq)}$, and the standard constant of the ion HSO_4^- in synthetic sea water from 273.15 to 318.15°K. J Chem Thermodyn 22:113–127

Dickson AG, Millero FJ (1987) A comparison of the equilibrium constants for the dissociation of carbonic acid in seawater media. Deep-Sea Res I 34:1733–1743

Dickson AG, Sabine CL, Christian JR (2007) Determination of the pH of sea water using the indicator dye m-cresol purple. In: Dickson AG, Sabine CL, Christian JR (eds) Guide to best practices for ocean CO_2 measurements. PICES Special Publication 3. IOCCP Rep 8. North Pacific Marine Science Organization, Sidney. http://cdiac.ornl.gov/oceans/Handbook_2007.html

Dlugokencky E, Tans P (2018) Trends in atmospheric carbon dioxide. National Oceanic & Atmospheric Administration, Earth System Research Laboratory (NOAA/ESRL). https://www.esrl.noaa.gov/gmd/ccgg/trends/data.html

Doney SC, Fabry VJ, Feely RA, Kleypas JA (2009) Ocean acidification: the other CO_2 problem. Annu Rev Mar Sci 1:169–192

Dorigan JL, Wilbur KM (1973) Calcification and its inhibition in coccolithophorids. J Phycol 9:450–456

Drenkard EJ, Cohen AL, McCorkle DC, de Putron SJ, Starczak VR, Zicht AE (2013) Calcification by juvenile corals under heterotrophy and elevated CO_2. Coral Reefs 32: 727–735

Feely RA, Alin SR, Newton J, Sabine CL and others (2010) The combined effects of ocean acidification, mixing, and respiration on pH and carbonate saturation in an urbanized estuary. Estuar Coast Shelf Sci 88:442–449

Flynn KJ, Blackford JC, Baird ME, Raven JA and others (2012) Changes in pH at the exterior surface of plankton with ocean acidification. Nat Clim Chang 2:510–513

Gledhill DK, White MM, Salisbury J, Thomas H and others (2015) Ocean and coastal acidification off New England and Nova Scotia. Oceanography 28:182–197

Green MA, Aller RC (1998) Seasonal patterns of carbonate diagenesis in nearshore terrigenous muds: relation to spring phytoplankton bloom and temperature. J Mar Res 56:1097–1123

Guillard RRL, Hargraves PE (1993) *Stichochrysis immobilis* is a diatom, not a chrysophyte. Phycologia 32:234–236

Hermoso M, Chan IZX, McClelland HLO, Heureux AMC, Rickaby REM (2016) Vanishing coccolith vital effects with alleviated carbon limitation. Biogeosciences 13: 301–312

Hinga KR (2002) Effects of pH on coastal marine phytoplankton. Mar Ecol Prog Ser 238:281–300

Hoppe CJM, Langer G, Rost B (2011) *Emiliania huxleyi* shows identical responses to elevated pCO_2 in TA and DIC manipulations. J Exp Mar Biol Ecol 406:54–62

Houlbrèque F, Reynaud S, Godinot C, Oberhänsli F, Rodolfo-Metalpa R, Ferrier-Pagès C (2015) Ocean acidification reduces feeding rates in the scleractinian coral *Stylophora pistillata*. Limnol Oceanogr 60:89–99

Iglesias-Rodriguez MD, Halloran PR, Rickaby REM, Hall IR and others (2008) Phytoplankton calcification in a high-CO_2 world. Science 320:336–340

IPCC (Intergovernmental Panel on Climate Change) (2014) Climate change 2014. Synthesis report. Intergovernmental Panel on Climate Change, Geneva

Irie T, Bessho K, Findlay HS, Calosi P (2010) Increasing costs due to ocean acidification drives phytoplankton to be more heavily calcified: optimal growth strategy of coccolithophores. PLOS ONE 5:e13436

Israel AA, González EL (1996) Photosynthesis and inorganic carbon utilization in *Pleurochrysis* sp. (Haptophyta), a coccolithophorid alga. Mar Ecol Prog Ser 137:243–250

Jin P, Ding J, Xing T, Riebesell U, Gao K (2017) High levels of solar radiation offset impacts of ocean acidification on calcifying and non-calcifying strains of *Emiliania huxleyi*. Mar Ecol Prog Ser 568:47–58

Krumhardt KM, Lovenduski NS, Freeman NM, Bates NR (2016) Apparent increase in coccolithophore abundance in the subtropical North Atlantic from 1990 to 2014. Biogeosciences 13:1163–1177

Langer G, Geisen M, Baumann KH, Kläs J, Riebesell U, Thoms S, Young JR (2006) Species-specific responses of calcifying algae to changing seawater carbonate chemistry. Geochem Geophys Geosyst 7:Q09006

Langer G, Nehrke G, Probert I, Ly J, Ziveri P (2009) Strain-specific responses of *Emiliania huxleyi* to changing seawater carbonate chemistry. Biogeosciences 6:2637–2646

LaRoche J, Rost B, Engel A (2010) Bioassays, batch culture and chemostat experimentation. In: Riebesell U, Fabry VJ, Hansson L, Gattuso JP (eds) Guide to best practices in ocean acidification research and data reporting. European Project on Ocean Acidification (EPOCA), Bremerhaven, p 81–94

Le Quéré C, Andrew RM, Friedlingstein P, Sitch S and others (2018) Global carbon budget 2017. Earth Syst Sci Data 10:405–448

Lewis MR, Smith JC (1983) A small volume, short-incubation-time method for measurement of photosynthesis as a function of incident irradiance. Mar Ecol Prog Ser 13:99–102

Li F, Wu Y, Hutchins DA, Fu F, Gao K (2016) Physiological responses of coastal and oceanic diatoms to diurnal fluctuations in seawater carbonate chemistry under two CO_2 concentrations. Biogeosciences 13:6247–6259

Linschooten C, van Bleijswijk JDL, van Emburg PR, de Vrind JPM, Kempers ES, Westbroek P, de Vrind-de Jong EW (1991) Role of the light-dark cycle and medium composition on the production of coccoliths by *Emiliania huxleyi* (Haptophyceae). J Phycol 27:82–86

Liu X, Patsavas MC, Byrne RH (2011) Purification and characterization of meta-cresol purple for spectrophotometric seawater pH measurements. Environ Sci Technol 45: 4862–4868

Marsh ME (1999) Coccolith crystals of *Pleurochrysis carterae*: crystallographic faces, organization, and development. Protoplasma 207:54–66

Marsh ME (2008) Regulation of coccolith calcification in *Pleurochrysis carterae*. In: Bäuerlein E (ed) Handbook of biomineralization: biological aspects and structure formation, Vol 1. Wiley-VCH, Weinheim p 211–226

McElhany P, Busch DS (2013) Appropriate pCO_2 treatments in ocean acidification experiments. Mar Biol 160: 1807–1812

Mehrbach C, Culberson CH, Hawley JE, Pytkowicz RM (1973) Measurement of the apparent dissociation constants of carbonic acid in seawater at atmospheric pressure. Limnol Oceanogr 18:897–907

Meyer J, Riebesell U (2015) Reviews and syntheses: responses of coccolithophores to ocean acidification: a meta-analysis. Biogeosciences 12:1671–1682

Moheimani NR, Borowitzka MA (2011) Increased CO_2 and the effect of pH on growth and calcification on *Pleurochrysis carterae* and *Emiliania huxleyi* (Haptophyta) in semicontinuous cultures. Appl Microbiol Biotechnol 90: 1399–1407

Monteiro FM, Bach LT, Brownlee C, Bown P and others (2016) Why marine phytoplankton calcify. Sci Adv 2: e1501822

Müller MN, Schulz KG, Riebesell U (2010) Effects of long-term high CO_2 exposure on two species of coccolithophores. Biogeosciences 7:1109–1116

Nimer NA, Merrett MJ (1993) Calcification rate in *Emiliania huxleyi* Lohmann in response to light, nitrate and availability of inorganic carbon. New Phytol 123:673–677

Orr JC, Fabry VJ, Aumont O, Bopp L and others (2005) Anthropogenic ocean acidification over the twenty-first century and its impact on calcifying organisms. Nature 437:681–686

Paasche E (1962) Coccolith formation. Nature 193:1094–1095
Paasche E (1964) A tracer study of the inorganic carbon uptake during coccolith formation and photosynthesis in the coccolithophorid *Coccolithus huxleyi.* Physiol Plant (Suppl III):1–82
Paasche E, Brubak S (1994) Enhanced calcification in the coccolithophorid *Emiliania huxleyi* (Haptophyceae) under phosphorus limitation. Phycologia 33:324–330
Parsons TR, Maita Y, Lalli CM (1984) A manual of chemical and biological methods for seawater analysis. Pergamon Press, New York, NY
Pierrot D, Lewis E, Wallace DWR (2006) MicroSoft Excel Program Developed for CO2 System Calculations, Oak Ridge Natl Lab, US Department of Energy, Carbon Dioxide Information Analysis Center, Oak Ridge, TN
Poulton AJ, Sanders R, Holligan PM, Adey T, Stinchcombe M, Brown L, Chamberlain K (2006) Phytoplankton mineralisation in the tropical and subtropical Atlantic Ocean. Glob Biogeochem Cycles 20:GB4002
Riebesell U, Zondervan I, Rost B, Tortell PD, Zeebe RE, Morel FMM (2000) Reduced calcification of marine plankton in response to increased atmospheric CO_2. Nature 407:364–367
Rivero-Calle S, Gnanadesikan A, Del Castillo CE, Balch WM, Guikema SD (2015) Multidecadal increase in North Atlantic coccolithophores and the potential role of rising CO_2. Science 350:1533–1537
Sokal RR, Rohlf FJ (1995) Biometry: the principles and practice of statistics in biological research. WH Freeman, New York, NY
Talmage SC, Gobler CJ (2010) Effects of past, present, and future ocean carbon dioxide concentrations on the growth and survival of larval shellfish. Proc Natl Acad Sci USA 107:17246–17251
Taylor AR, Chrachri A, Wheeler G, Goddard H, Brownlee C (2011) A voltage-gated H+ channel underlying pH homeostasis in calcifying coccolithophores. PLOS Biol 9: e1001085
Taylor AR, Brownlee C, Wheeler GL (2012) Proton channels in algae: reasons to be excited. Trends Plant Sci 17: 675–684
Uppström LR (1974) The boron/chlorinity ratio of deep-sea water from the Pacific Ocean. Deep Sea Res I 21:161–162
van der Wal P, deVrind JPM, de Vrind-de Jong EW, Borman AH (1987) Incompleteness of the coccosphere as a possible stimulus for coccolith formation in *Pleurochrysis carterae* (Prymnesiophyceae). J Phycol 23:218–221
Waldbusser GG, Salisbury JE (2014) Ocean acidification in the coastal zone from an organism's perspective: multiple system parameters, frequency domains, and habitats. Annu Rev Mar Sci 6:221–247
Waldbusser GG, Brunner EL, Haley BA, Hales B, Langdon CJ, Prahl FG (2013) A developmental and energetic basis linking larval oyster shell formation to acidification sensitivity. Geophys Res Lett 40:2171–2176
Wallace RB, Baumann H, Grear JS, Aller RC, Gobler CJ (2014) Coastal ocean acidification: the other eutrophication problem. Estuar Coast Shelf Sci 148:1–13
Winter A, Henderiks J, Beaufort L, Rosalind EM, Rickaby REM, Brown CW (2014) Poleward expansion of the coccolithophore *Emiliania huxleyi*. J Plankton Res 36: 316–325
Wolf-Gladrow DA, Zeebe RE, Klaas C, Kortzinger A, Dickson AG (2007) Total alkalinity: the explicit conservative expression and its application to biogeochemical processes. Mar Chem 106:287–300

Editorial responsibility: Katherine Richardson, Copenhagen, Denmark

Submitted: November 2, 2017; Accepted: May 14, 2018
Proofs received from author(s): July 31, 2018